Materials Science and Engineering A 538 (2012) 63–68

Contents lists available at SciVerse ScienceDirect

Materials Science and Engineering A

journal homepage: www.elsevier.com/locate/msea

Mechanisms of grain refinement in Mg–6Al–1Zn alloy during hot deformation

H. Miura[a,*], M. Ito[a], X. Yang[b], J.J. Jonas[c]

[a] Department of Mechanical Engineering and Intelligent Systems, UEC Tokyo (The University of Electro-Communications), Chofu, Tokyo 182-8585, Japan
[b] School of Materials Science and Engineering, Central South University, Changsha 410083, China
[c] Department of Materials Engineering, McGill University, Montreal, Quebec H3A 2B2, Canada

ARTICLE INFO

Article history:
Received 26 October 2011
Received in revised form
19 December 2011
Accepted 9 January 2012
Available online 16 January 2012

Keywords:
Magnesium alloy
Dynamic recrystallization
Grain refinement
Twin
Kink
High temperature deformation

ABSTRACT

Mechanisms of grain refinement were investigated in an extruded Mg–6Al–1Zn alloy during hot compression at 623 K and a true strain rate of 3×10^{-3} s^{-1}. With increasing strain, grain fragmentation gradually took place; the dominant grain refinement mechanism, however, depended on the strain. At strains up to $\varepsilon = 0.1$, mechanical twinning contributed notably to grain refinement and to the formation of high angle boundaries. At medium to high strains, continuous dynamic recrystallization took place. Kinking contributed to grain fragmentation at all strains. The latter two mechanisms also increased the fraction of low to medium angle boundaries.

1. Introduction

It is well known that continuous dynamic recrystallization (cDRX) is one of the most important DRX mechanisms in Mg and Mg alloys [1,2]. According to this mechanism, low angle boundaries are introduced as a result of the gradual increase in misorientation at sub-boundaries due to the accumulation of dislocations. In short, deformation and recovery processes are responsible for the evolution of new grains. It has also been reported that heterogeneous deformation microstructures can also contribute to grain fragmentation. For example, Al-Samman and Gottstein reported that new DRX grains form next to mechanical twins [3], although they concluded that twinning itself is not a DRX mechanism. Conversely, Sitdikov and Kaibyshev [4], and Miura et al. [5] maintain that twinning as well as kinking are important mechanisms of DRX in Mg alloys. Although the roles of these heterogeneous deformation microstructures on grain fragmentation are evident, further research is necessary for a clear understanding of DRX mechanisms in Mg alloys.

When extensive DRX takes place, it is usually accompanied by work softening in cubic materials [6]. This type of softening, however, is usually absent when cDRX is the dominant DRX mechanism [7]. Nevertheless, work softening is sometimes reported even in Mg alloys. Such softening could theoretically be caused by crystal rotations that induce easy slip, which then results in softening [8]. The latter is generally referred to as "geometric softening". In this case, the peak strain does not depend on the deformation temperature or strain rate.

As briefly outlined above, the DRX mechanisms operating in Mg alloys differ from those taking place in cubic materials. The purpose of the present study was to investigate grain refinement mechanisms in Mg alloys during hot compression by means of orientation imaging microscopy (OIM).

2. Experimental

A commercial hot-extruded Mg AZ61 alloy was homogenized at 733 K for 2 h to achieve an initial grain size of 80 μm (Fig. 1). The rod was spark cut into rectangular samples with dimensions of 33 mm × 22.5 mm × 15 mm. The samples were deformed in compression in a vacuum on an Instron-type mechanical testing machine at 623 K at a true strain rate of 3×10^{-3} s^{-1}. The loading axis was parallel to the extrusion axis. Hot compression to various strains was followed by water quenching within 1 s to minimize the microstructural changes. Subsequently, the evolved microstructure was observed on a plane parallel to the compression axis using OIM.

* Corresponding author. Tel.: +81 42 443 5409; fax: +81 42 484 3327.
E-mail addresses: miura@mce.uec.ac.jp (H. Miura), yangxuyue@mail.csu.edu.cn (X. Yang), john.jonas@mcgill.ca (J.J. Jonas).

0921-5093/$ – see front matter
doi:10.1016/j.msea.2012.01.014

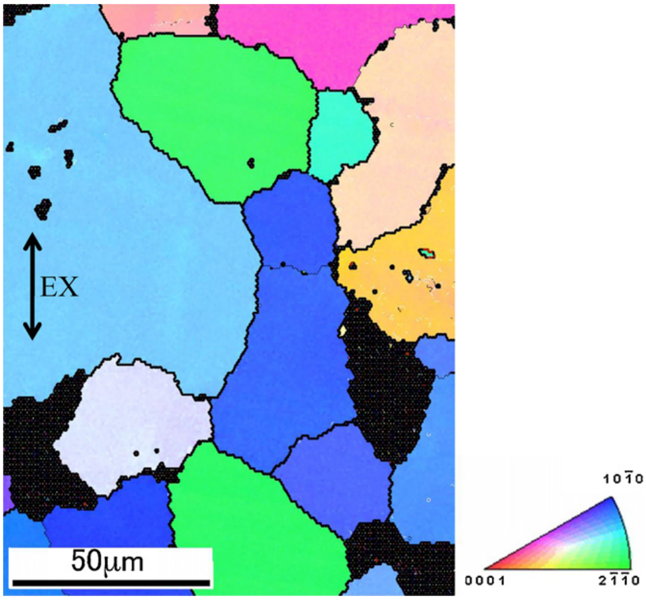

Fig. 1. Initial microstructure before hot deformation. EX indicates direction of extrusion, which is parallel to the compression axis. Colors indicate the crystallographic direction parallel to the compression axis. (For interpretation of the references to color in this figure legend, the reader is referred to the web version of this article.)

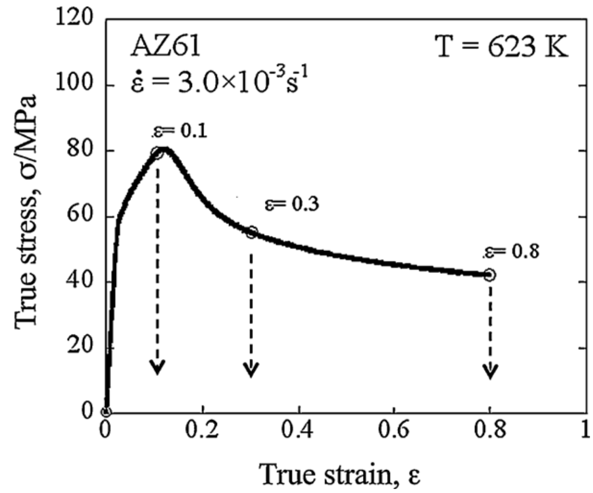

Fig. 2. True stress vs. true strain curve obtained by hot compression of the AZ61Mg alloy at 623 K and a true strain rate of 3×10^{-3} s^{-1}. Samples were water quenched at the strains indicated by the arrows.

3. Results

A typical true stress vs. true strain curve produced by hot deformation is illustrated in Fig. 2. The presence of a well-defined peak followed by appreciable work softening should be noted. The flow stress is reduced to almost half by the softening. Compression was terminated at the strains indicated by the arrows, i.e., at the peak strain, after the considerable work softening and in the steady-state region. Such peak stresses followed by work softening are usually caused by the extensive occurrence of DRX in cubic materials [6,7]. Because DRX is a thermally activated process, the peak strain

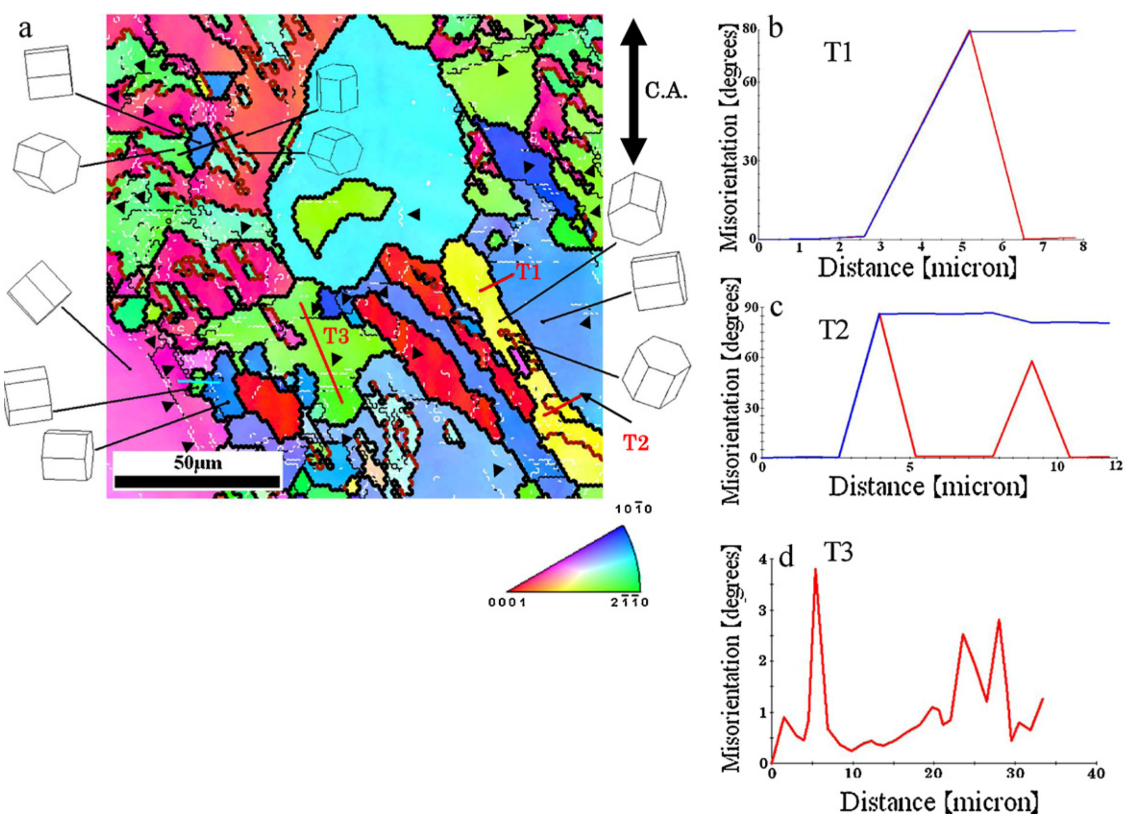

Fig. 3. (a) Microstructure present at a strain of $e = 0.1$. Unit cells representing twins are shown in some areas. Thin and bold black lines indicate low $3^\circ \leqq \theta < 15^\circ$ and high $15^\circ < \theta$ angle boundaries, respectively. The thin white and bold brown lines are $\theta < 3^\circ$ sub-boundaries and twin boundaries, respectively. Some kink bands are indicated by triangular marks. Disorientation changes along the T_1, T_2 and T_3 lines are presented in (b), (c), and (d), respectively. Red and blue lines in (b)–(d) show the disorientation of point-to-point and point-to origin. Color coding as in Fig. 1. (For interpretation of the references to color in this figure legend, the reader is referred to the web version of this article.)